

The *IUE* Absorption Spectrum of the Nucleus of NGC 246: Mostly C IV and O VI

WALTER A. FEIBELMAN¹

Laboratory for Astronomy and Solar Physics, Code 684.1, NASA-Goddard Space Flight Center, Greenbelt, Maryland 20771
 Electronic mail: SMTP%"feibelman@iue.nasa.gsfc.gov"

Received 1995 February 2; accepted 1995 March 6

ABSTRACT. We present a list of more than 140 absorption features and their equivalent widths for the central star of the planetary nebula NGC 246 as observed in the wavelength range $\lambda 1169$ – $\lambda 2000$. High signal-to-noise ratios are achieved by coadding nine high-dispersion SWP spectra, representing a total of nearly 22 hr observing time. The *IUE* spectrum is dominated by strong absorption lines, or blends, of O VI and C IV. Other ions include N V, O V, Si IV, Fe VI, Fe VII, and Ne VII, plus interstellar absorption lines. The only feature to display a P Cygni profile is the C IV resonance doublet from which a terminal wind velocity of 4120 ± 200 km s⁻¹ is derived.

1. INTRODUCTION

The central star of the planetary nebula NGC 246 (118.8–74.7 in the Acker et al. 1992 designation) is one of the hottest planetary nebula nuclei (PNN) known and presents an important object for studying the characteristics of hydrogen-deficient stars. Because NGC 246 is relatively bright, it is well suited for observations in the high-resolution (0.1 Å) mode of the *IUE* SWP range.

The nucleus (hereafter referred to simply as NGC 246) has been studied extensively at other wavelengths. It has a Wolf–Rayet type spectrum and belongs to the rare class of stars that show strong O VI emission lines in the optical region near $\lambda 3811$, $\lambda 3838$ (Smith and Aller 1969). It is also an EUV source. Furthermore, Werner and Rauch (1994) identified the permitted $\lambda 3643.6$ absorption as the only Ne VII transition, $2s3s-2s3p\ ^1S-^1P^0$, in the optical spectrum of NGC 246. A triplet of Ne VII is found in the ultraviolet region at $\lambda 11982.0$, $\lambda 11992.1$, and $\lambda 11997.3$ and falls into the range of the SWP camera where echelle ripple effects and an interorder break tend to be troublesome. The UV lines are listed by Kelly (1987) as $\lambda 11981.974$, $\lambda 11992.060$, and $\lambda 11997.345$, with relative intensities of 600, 300, and 100, respectively. The wavelengths were originally given by Bockasten et al. (1963) with estimated errors of 0.010 Å.

Besides showing high ionization features of C IV, O VI, and Ne VII, NGC 246 is one of only about a dozen PNe that are confirmed X-ray sources (Apparao and Tarafdar 1989). An early *IUE* high-dispersion spectrum (SWP 3353) taken during the *IUE* commissioning period (Heap 1982) displayed a weak P Cyg profile for the C IV resonance doublet in NGC 246, indicative of a stellar wind but no P Cyg lines are seen for H lines or other species in the optical region. In a study of four PG 1159-type stars by Werner et al. (1991), NGC 246 was singled out as a prime candidate for careful analysis using model atmospheres including C and O, particularly because NGC 246 (at that time) was considered to be a non-

pulsating optical spectroscopic twin to the central star of KI-16 but has recently been found to show pulsations similar to PG 1159–035 (Bond and Ciardullo, private communication). Again, because of its relative brightness in the *IUE* range, NGC 246 presents an ideal opportunity to study an UV spectrum of a very hot object dominated by C IV and O VI transitions. A recent line list of more than 130 transitions of C IV and O VI in the wavelength region $\lambda 1100$ – $\lambda 2000$ by Feibelman and Johansson (1995) permits identification of numerous stellar- absorption features belonging to these ions in the SWP spectrum of NGC 246.

No nebular emission lines were detected in the *IUE* spectrum of NGC 246 since the large (245" diameter nebula falls outside of the 10"×23" entrance aperture of the SWP camera. Interstellar (and possibly circumstellar) lines of N I, Fe II, S II, Si II, Si III, C I, C II, O I, Al II, and Al III are identified.

The following stellar parameters for NGC 246 are given by Acker et al. (1992): $V=11.96$; spectral type: WC-O VI; systemic radial velocity: -46.0 ± 6.6 ; diameter of nebula: 245"; distance: 0.47 kpc. From the strength of the Ne VII $\lambda 3644$ line, Werner and Rauch (1994) estimate $T_{\text{eff}} > 130,000$ K and also determined a high ($\sim 2\%$ by mass) neon abundance. Husfeld (1987) determined $\log g = 5.6$ for NGC 246.

2. OBSERVATIONS

The *IUE* archives contain nine suitable short-wavelength (SWP) high-dispersion spectra of NGC 246. All were taken through the large (10"×23") entrance aperture, centered on the nucleus. These spectra (SWP 3353, 41997, 42068, 42073, 42104, 42214, 42247, 47843, and 47844) were used for an exposure-weighted coadded spectrum covering the spectral range $\lambda 1175$ – $\lambda 1925$ shown in Fig. 1. No significant absorptions were detected between $\lambda 1925$ and $\lambda 1980$. An additional section $\lambda 1980$ – $\lambda 2000$ spanning the Ne VII triplet $\lambda 11982$, 1992, 1997 required special processing to extract additional useful data because of an echelle interorder gap of about 5 Å. The C IV feature near $\lambda 1169$ was also measured but is not included in Fig. 1 since the sensitivity of the SWP camera falls off steeply shortward of $\approx \lambda 1170$.

¹Guest observer with the International Ultraviolet Explorer (*IUE*) satellite which is sponsored and operated by the National Aeronautics and Space Administration, by the European Space Agency, and by the Science and Engineering Research Council of the United Kingdom.

3. DATA REDUCTION

We used the interactive computer routine *FEATURE* available at the Goddard Data Analysis Center (*IUEDAC*) to measure wavelengths and equivalent widths of absorption features. The wavelengths shown represent the centroid of the absorption features that are often blends of two or more lines. They are displayed by the computer to three significant figures which were then rounded off to two figures to give wavelengths accurate to better than 0.1 Å for narrow, unblended features.

Equivalent widths (EW) were determined by the same routine and are estimated to be accurate to $\pm 10\%$ unless otherwise noted. For marginally exposed *IUE* spectra the interorder background noise can result in erroneous EW but for the NGC 246 spectra this is not a problem since the stellar continuum level is well exposed, as seen in Fig. 1, and no saturation occurs for C IV or O VI lines. For the C IV $\lambda\lambda 1351, 1352$ blend the assumption was made that the continuum level halfway between the blended absorptions determines the EW. The overlapping lines of C IV and O VI in the regions near $\lambda 1637$ and $\lambda 1641$, as well as some blends with

Fe VI or interstellar lines cannot be deconvolved into separate transitions so that only approximate values for the blended lines are shown.

The Ne VII triplet falls into a difficult region of high dispersion *IUE* spectra, $\lambda 1980$ – $\lambda 2000$, where linearity of the detectors diminish and an interorder echelle gap of 5 Å exists. In addition, calibrations from laboratory data change from vacuum to air wavelengths at 2000 Å. The region of interest was therefore recalibrated to make sure that all spectra were compared to UV wavelength standards. The $\lambda 1982.0$ line is in echelle order number 70 while the $\lambda\lambda 1992.1, 1997.3$ lines are in order number 69. A reseau mark is present on all spectra near $\lambda 1994.5$. Although Ne VII represents the highest stage of ionization seen in *IUE* spectra of central stars, these absorptions show the largest equivalent widths of any lines in NGC 246 and suggest its neon-rich nature. Some weak, unidentified lines are present in this region.

Radial velocities were also determined for the strongest lines, or blends of lines, by the computer routine *FEATURE*.

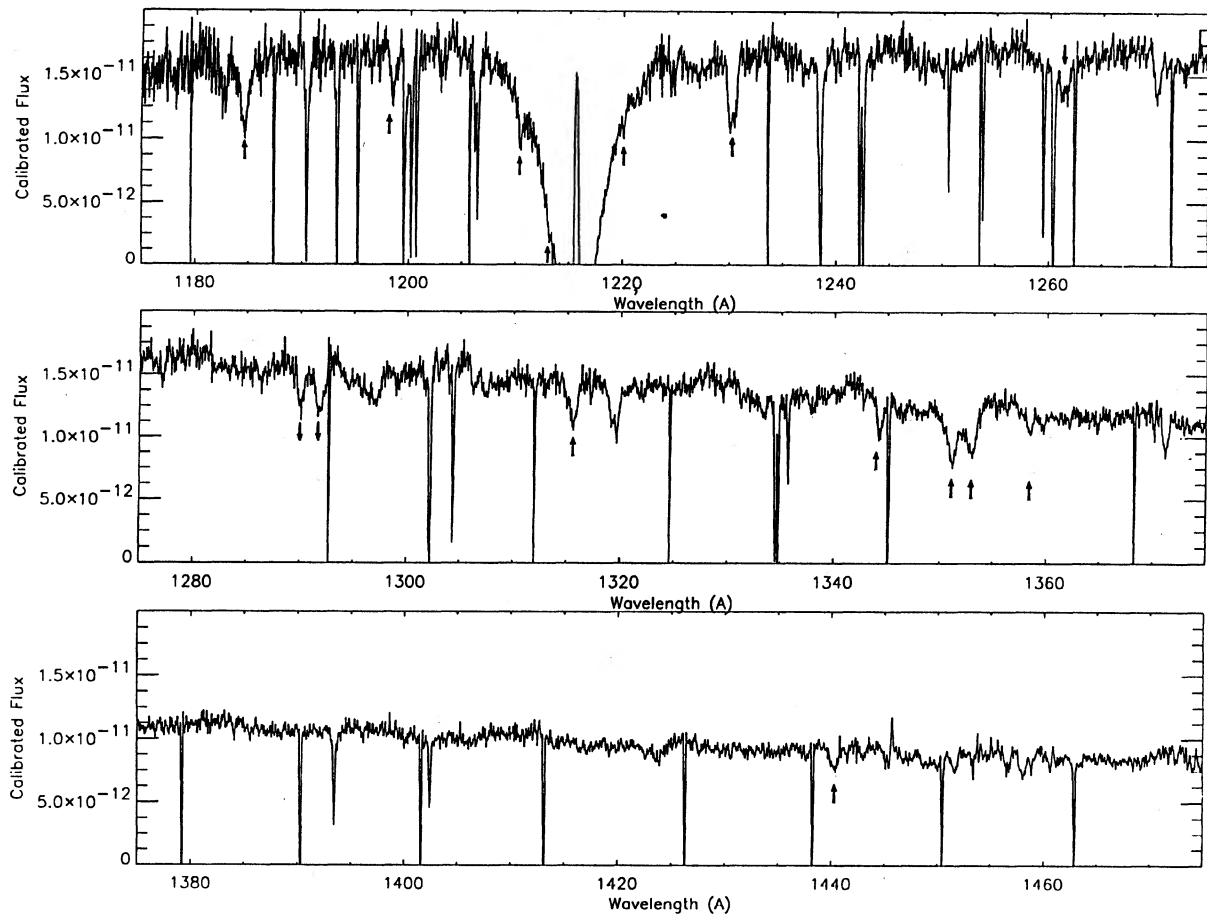


FIG. 1—The *IUE* high-resolution spectrum of NGC 246, covering the wavelength range $\lambda 1175$ – $\lambda 1920$. The tracing consists of nine exposure-weighted coadded spectra. Each panel covers 100 Å. Notice change of vertical scale for every third panel. The spectrum was smoothed by a three-point running average. Strong C IV absorptions are marked \uparrow and strong O VI are marked \downarrow .

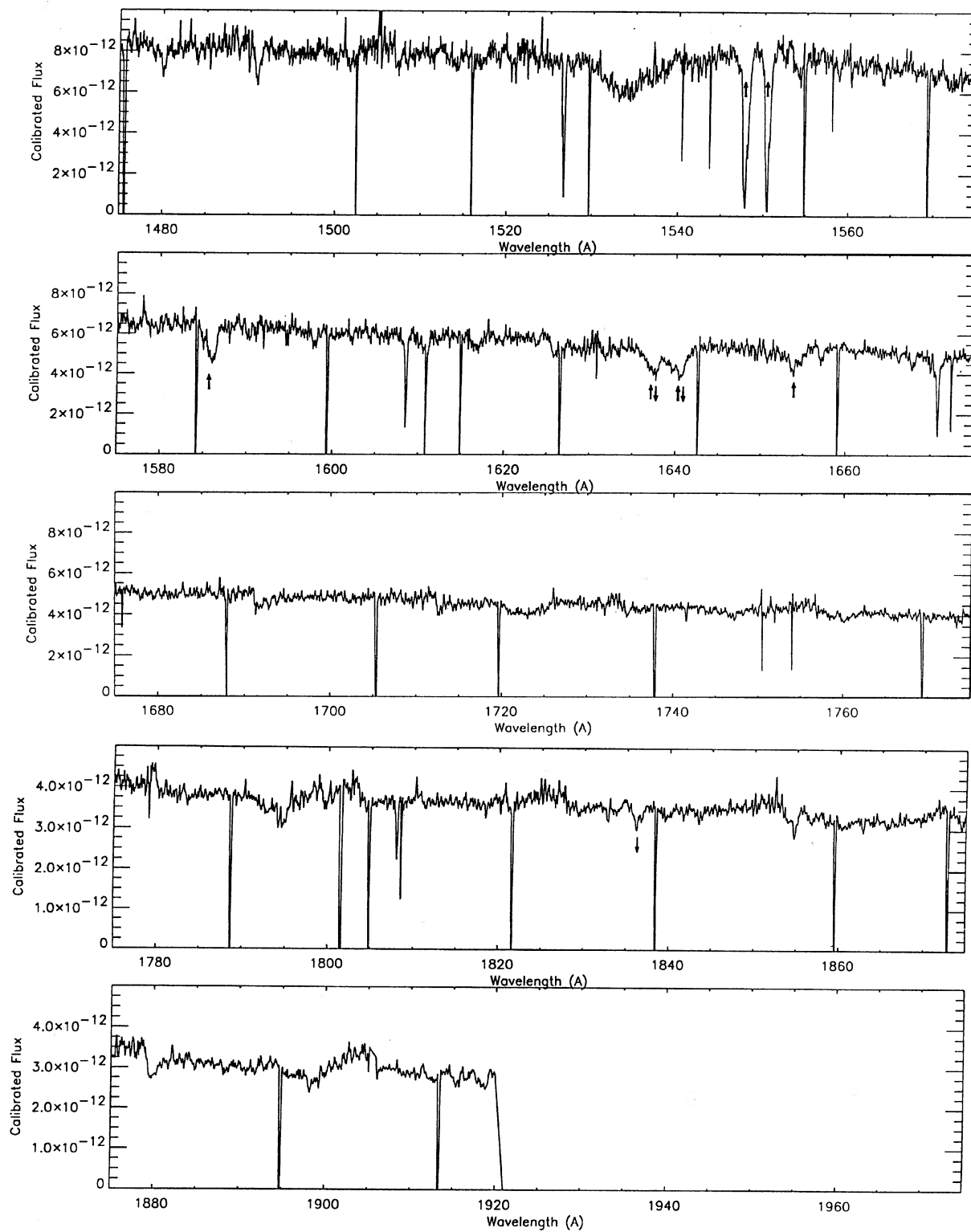


FIG. 1—(Continued)

TABLE I
 Absorption Features in NGC 246 Nucleus from Nine Coadded SWP Spectra

λ (obs.,Å) (centroid) ^a	λ (lab) (Å)	Ion	Refer- ence ^b	Equivalent Width (mÅ)	Radial Velocity (km s ⁻¹)	Entry #	Comments	λ (obs.,Å) (centroid) ^a	λ (lab) (Å)	Ion	Refer- ence ^b	Equivalent Width (mÅ)	Radial Velocity (km s ⁻¹)	Entry #	Comments
(1)	(2)	(3)	(4)	(5)	(6)	(7)	(8)	(1)	(2)	(3)	(4)	(5)	(6)	(7)	(8)
1168.76	1168.847 1168.990	C IV C IV	1 1	306	-23.1	1 2	blend	1306.23	1306.60	Ni V ?	2	28:	..	63	blend?
1170.91	1171.562	O VI	1	148	-23.2	3		1308.62	1308.645	Fe VI	5	10:	-3.6	64	I = 500°
1172.10	1172.439	O VI	1	59	?	4		1315.51	1315.625 1315.852	C IV C IV	1 1	165	-24.0	65 66	blend
1184.59	1184.590 1184.774	C IV C IV	1 1	298	-20.0	5 6	blend	1317.68	1317.736	Fe VI	5	29	(-11.8)	67	I = 400°
1190.43	1190.426	Si II	2	224	1.2	7	ISM	1319.14	?	?		102	..	68	blend
1191.48	1191.327	O VI	1	9:	..	8	see text	1319.69	?	?		115	..	69	
1191.66	?	?		15:	..	9		1328.81	1328.833	C I	2	11:	-5.3	70	ISM
1193.02	?	?		28	..	10	blend	1328.81	1329.100	C I	2	11:	..	71	blend
1193.29	1193.290	Si II	2	205	4.6	11	ISM	1329.172	1329.172	Fe VI	5	11:	..	72	I = 500°
1198.43	1198.403 1198.554 1198.591	C IV C IV C IV	1 1 1	80	-28.9	12 13 14	blend	1332.08	1332.381	Fe VII	4	13:	..	73	doubtful
1199.57	1199.549	N I	2	212	0.6	15	ISM	1334.52	1334.532	C II	3	218	-1.2	74	ISM
1199.83	1199.908	C IV	1	25	(-23.8)	16	blend	1335.37	1335.707	C II	3	17:	..	75	ISM
1200.22	1200.097 1200.224	C IV N I	1 2	163	0.6	17 18	blend ISM	1335.71	1335.708	C II	3	94	-0.6	76	ISM
1200.73	1200.711	N I	2	162	2.0	19	ISM	1335.25	1336.148	O VI	1	77	too weak
1206.36	1206.510	Si III	3	242	-7.4 -76.5 (-145.0)	20 21 22	ISM 2nd part 3rd ?	1336.84	1336.843	Fe VI	5	7:	(-30.0)	78	I = 250°
1207.96	1208.375	Fe VII	4	24:	?	23	see text	1337.93	1337.695 1337.788	Fe VI Fe VI	5 5	7:	6.3	79 80	I = 250, 400° blend
1210.49	1210.614 1210.649	C IV C IV	1 1	39	-30.1	24 25	in Ly- α trough	1338.65	1338.612	O IV	2	7:	6.7	81	ISM
1213.52	1213.502 1213.561	C IV C IV	1 1	55	(-12.5)	26 27	in Ly- α trough	1342.78	1343.510	O IV	2	19:	..	82	
1219.81	1219.816 1219.875	C IV C IV	1 1	10:	(-15.7)	28 29	in Ly- α trough	1344.36	1344.178 1344.415	C IV C IV	1 1	141	-22.3	83 84	blend
1226.42	1226.653	Fe VII	4	16:	?	30	doubtful	1351.07	1351.216 1351.289	C IV C IV	1 1	493	-26.9	85 86	blend
1230.00	1230.043	C IV	1	165	-20.8	31	blend	1352.91	1352.975 1353.429	C IV C IV	1 1	381	-23.2	87 88	blend
1230.19	1230.521	C IV	1	106		32		1358.45	1358.424 1358.469 1358.498	C IV C IV C IV	1 1 1	72	(-0.9)	89 90 91	blend
1232.47	1232.479	Fe VI	5	21	(-1.1)	33	I = 300°	1402.	1402.623 1402.770	O VI Si IV	1 3	110	-70.4	95 96	blend ISM
1238.52	1238.821	N V	3	349	-66.5	34		1413.	1413.388 1413.667	O VI O VI	1 1	9:	..	97 98	in reseau
1239.92	1239.690	Fe VII	4	15:	?	35	doubtful	1423.56	1423.366 1423.367	O VI O VI	1 1	12:	..	99 100	blend
1242.64	1242.804	N V	3	223	-63.3	36		1425.11	1425.314	O VI	1	11:	..	101	too weak
1250.59	1250.586	S II	2	103	-0.5	37	ISM	1440.27	1440.283 1440.364	C IV C IV	1 1	102	-19.4	102 103	blend
1253.81	1253.812	S II	2	125	-0.7	38	ISM	1526.68	1526.707	Si II	2	243	0.0	104	ISM, split
1259.52	1259.520	S II	2	148	-0.6	39	ISM, blend	1545.39	1545.285	O VI	1	18:	..	105	too weak
1260.44	1260.418 1260.736	Si II C I	2 2	292	1.3	40 41	in O VI blend with	1547.90	1548.187	C IV	1	715	-66.0	106	see text
1261.	1261.766 1262.148	O VI O VI	1 1	(462)	..	42 43	S II, Si II, and reseau removed see text for Fe VI	1550.48	1550.772	C IV	1	619	-66.5	107	see text
1266.11	1266.103	Fe VI	5	19:	-0.7	44	I = 500°	1560.33	1560.310	C I	2	29	-2.9	108	ISM
1270.16	1270.408	C I	3	149	(-48.5)	45	broad, ISM	1561.05	1560.683	C I	2	8:	..	109	ISM
1276.69	1276.797	O VI	1	13:	-24.8	46		1585.96	1585.811 1586.111 1586.141	C IV C IV C IV	1 1 1	247	-26.9	110 111 112	blend
1277.13	1277.245 1277.513	C I C I	3 3	44	-7.1	47 48	ISM blend	1608.46	1608.208 1608.456	O VI Fe II	1 3	113 114	blend ISM
1278.31	1278.291	Fe VI	5	8:	(-8.0)	49	I = 600°	1637.37	1637.543 1637.650	C IV C IV	1 1	249	(-19.7)	115 116	blend see text
1280.21	1280.135	C I	2	9:	..	50	doubtful	1638.	1638.109	O VI	1			117	
1290.02	1289.807	O VI	1	80	(28.0)	51		1640.06	1640.098	C IV	1	379	(-43.6)	118	blend
1291.82	1291.923 1292.041 1292.842 1293.243	O VI O VI O VI O VI	1 1 1 1	255	-18.5	52 53 54 55	4 blended lines	1641.	1641.031 1641.063	C IV C IV	1 1			119 120	see text
1295.73	1295.572	O VI	1	23	..	56	blend	1641.	1641.201	O VI	1			121	
1295.78	1295.813	Fe VI	5	18:	-6.9	57	I = 300°	1649.47	1649.539 1649.920	O VI O VI	1 1	15:	-32.9	122 123	blend
1301.68	1301.796	Fe VI	5	7:	(-5.5)	58	I = 600°	1653.63	1653.633 1653.992	C IV C IV	1 1	62	-28.9	124 125	blend
1302.18	1302.169 1302.439	O I O VI	3 1	258	5.8	59	ISM blend	1654.60	1654.457 1654.564 1654.566	C IV C IV C IV	1 1 1	27:	..	126 127 128	blend
1302.97	?	?		15:	..	60									
1303.96	1303.781	O VI	1	33		61	ISM blend								
1304.37	1304.369	Si II	2	168	0.5	62	ISM								

TABLE 1
(Continued)

λ (obs., Å) (centroid) ^a	λ (lab) (Å)	Ion	Refer- ence ^b	Equivalent Width (mÅ)	Radial Velocity (km s ⁻¹)	Entry #	Comments
(1)	(2)	(3)	(4)	(5)	(6)	(7)	(8)
1657.03	1656.266	C I	2	36	..	129	blend, ISM
	1656.928	C I	2			130	ISM
	1657.380	C I	2			131	ISM
	1657.907	C I	2			132	ISM
1670.77	1670.787	Al II	2	349	3.4	133	ISM
1717.33	?	?		29	..	134	
1718.56	1718.551	N IV	2	11:	1.4	135	
1808.02	1808.003	Si II	2	86	5.7	136	ISM
1836.73	1836.885	O VI	1	15:	-28.6	137	
1854.81	1854.716	Al III	3	78	-2.8	138	ISM
1862.80	1862.789	Al III	3	27:	..	139	ISM
1936.14	1936.333	O VI	1	26:	..	140	doubtful
1981.84	1981.974	Ne VII	6	326	20.1	141	9 coadded
1991.94	1992.060	Ne VII	6	335	16.7	142	3 best
1997.26	1997.345	Ne VII	6	192	20.9	143	9 coadded

^acentroid of absorption feature as measured with interactive computer routine FEATURE.

^bReferences for rest wavelengths are: 1 = Feibelman & Johansson (1995); 2 = Dean & Bruhweiler (1985); 3 = Morton (1991); 4 = Ekberg (1981); 5 = Ekberg (1975b); 6 = Kelly (1987)

} means unresolved fine structure

^cIntensities shown for Fe VI are from Ekberg (1975b)

4. DISCUSSION

The absorption features in the *IUE* spectrum of NGC 246 are listed in Table 1. Column (1) gives the observed wavelength of the centroid; column (2) the laboratory rest wavelength in Å; column (3) the ion identification; column (4) the

reference for each of the identifications; column (5) the equivalent width in mÅ; column (6) the measured radial velocity; column (7) the running entry number; and column (8) some comments to identify interstellar lines, blends, and intensities of Fe VI lines from Ekberg (1975b).

Identification of the C IV and O VI lines are from Feibelman and Johansson (1995), interstellar lines from Dean and Bruhweiler (1985), resonance absorptions from Morton (1991), Fe VII lines from Ekberg (1981), Fe VI lines from Ekberg (1975b), and Ne VII lines from Kelly (1987). Reference to Fe V lines in the text come from Ekberg (1975a).

Absorption features marked by } represent unresolved fine structure transitions. A colon (:) after the equivalent width means that the measurement has large errors, $\pm 50\%$, due to the weakness of the absorption feature. A large number of features, primarily Fe VI lines, whose EW are less than 15 mÅ are not shown. Radial velocities with large uncertainties are shown in parentheses () and may be as large as $\pm 25\%$; the nominal accuracy for a well-exposed high-dispersion spectrum is $\pm 3 \text{ km s}^{-1}$ internal to the same image.

4.1 The C IV and O VI Absorptions

The UV spectrum of NGC 246 is dominated by strong and broadened absorptions of highly excited C IV and O VI transitions that in some places overlap and are also superposed on interstellar lines and very weak absorption lines of Fe VI.

The broad absorptions ($\Delta\lambda \approx 7 \text{ Å}$) near $\lambda 1640$ are of particular significance since they could easily be attributed to He II in low-dispersion spectra. The high-dispersion data

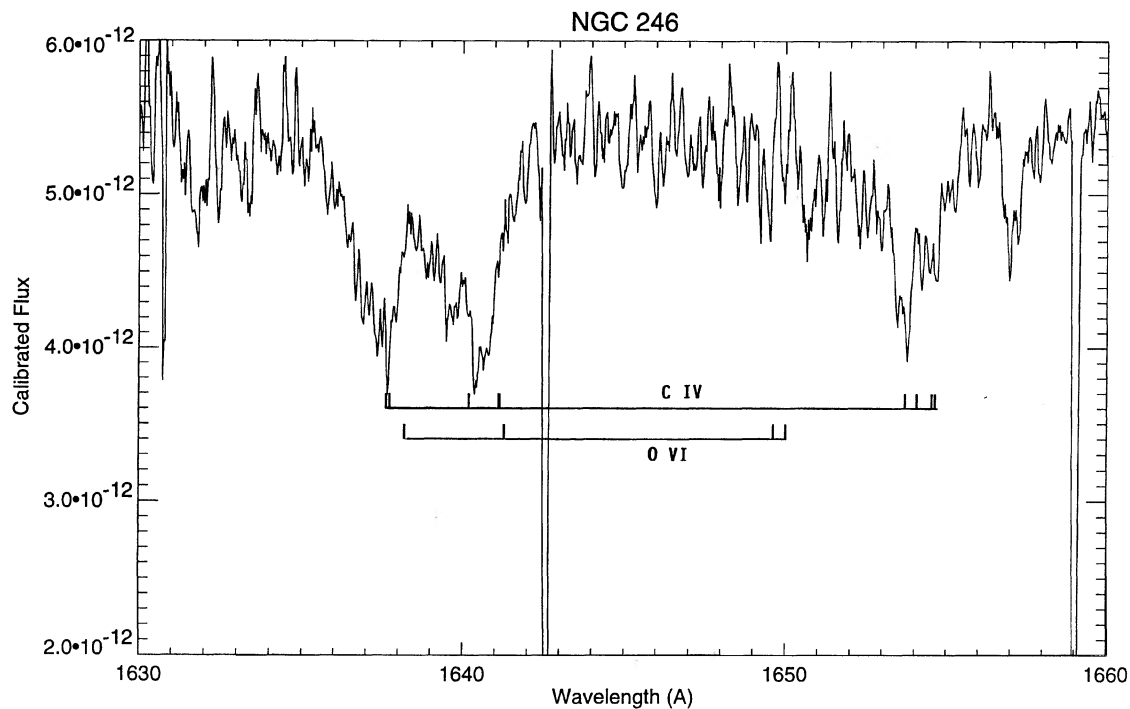


FIG. 2.—The region near $\lambda 1640$ in the spectrum of NGC 246. The high-dispersion spectrum clearly demonstrates that overlapping absorptions of C IV and O VI are responsible for a broad, asymmetric trough that could easily be interpreted in low-resolution spectra as being due to He II $\lambda 1640.4$. The zero level has been suppressed to show detail.

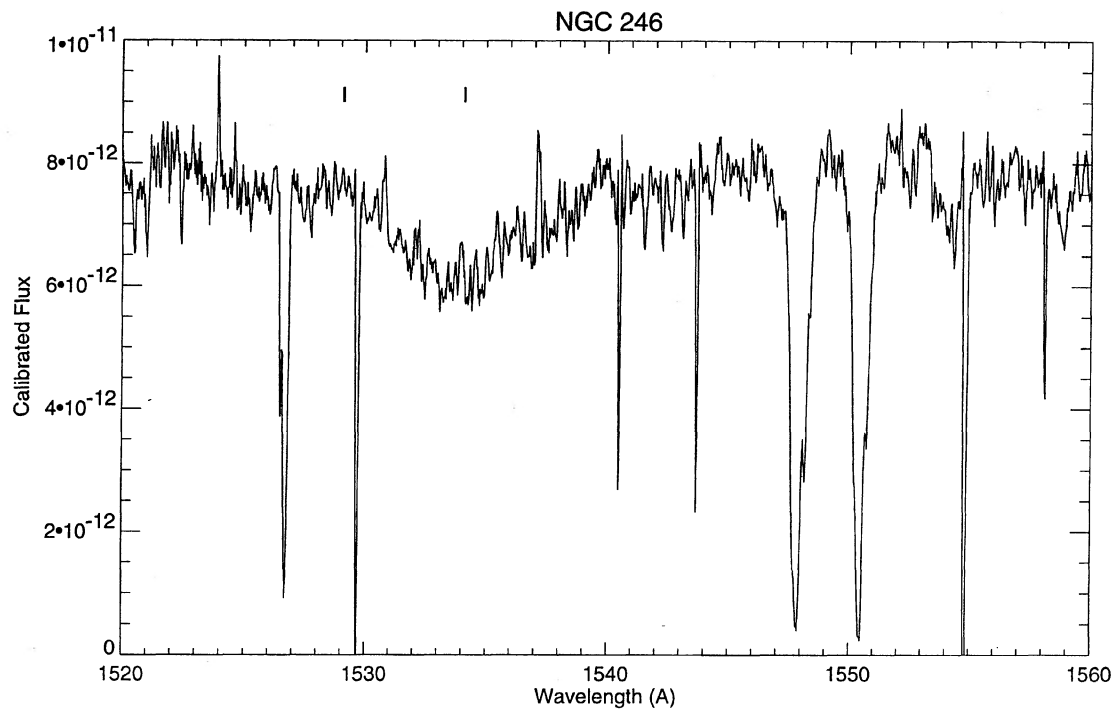


FIG. 3—The P Cygni profile of the C IV resonance doublet in NGC 246. The emission component is quite weak and the absorption is unusual in that the deepest part occurs near ν_{∞} rather than near the longward end. A terminal velocity of $4120 \pm 200 \text{ km s}^{-1}$ is derived from ν_{∞} . Several weak unidentifiable absorption lines are also present.

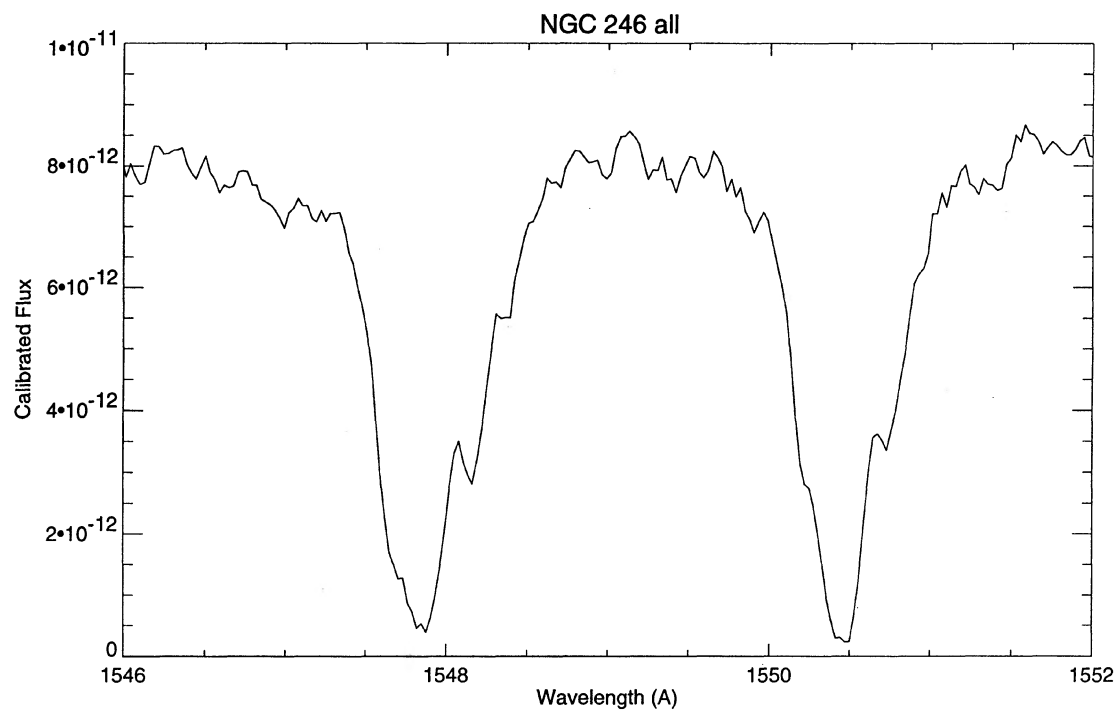


FIG. 4—The narrow C IV absorptions within the broad P Cyg profile of the C IV resonance lines for NGC 246. Notice the weak secondary components at -10 km s^{-1} from the rest wavelengths of each main absorption feature at -66 km s^{-1} .

clearly show that for NGC 246 overlapping absorptions of C IV and O VI are responsible for the features shown in Fig. 2.

4.2 The P Cyg Profile of C IV and Terminal Wind Velocity

A weak P Cyg profile for the resonance doublet of C IV was mentioned by Heap (1982), based on the single SWP 3353 high-dispersion spectrum. The nine coadded spectra indicate this P Cyg C IV feature more convincingly, as shown in Fig. 3 where two tic marks indicate the terminal wind velocity, v_∞ , and the "black" edge velocity, v_b . We derive a terminal wind velocity of $4120 \pm 200 \text{ km s}^{-1}$ from v_∞ (and a black edge velocity of $2700 \pm 250 \text{ km s}^{-1}$), clearly showing that mass loss is occurring in NGC 246. The profile is unusual in that the emission component is very weak and the deepest part of the absorption occurs near v_∞ rather than near the emission component, suggesting strong turbulence. Additional unidentifiable absorptions are seen that are reminiscent of those in Abell 78 (Kaler et al. 1988) but their spacings do not match the 2.6 \AA separation of the rest wavelengths of the C IV doublet.

The narrow C IV absorptions also show a secondary absorption in both components. These are displaced by -10 km s^{-1} from the rest wavelengths while the main features are at -66 km s^{-1} , as shown in greater detail in Fig. 4.

4.3 Absorption Features of Fe VI and Fe VII

As was indicated by Schönberner and Drilling (1985), in most of their hottest program stars only the strongest Fe V lines appear to be present; it was shown in their illustrations

that Fe V and Fe VI lines are quite strong in stars whose $T_{\text{eff}}=60,000\text{--}80,000 \text{ K}$, and that Fe V lines rapidly diminish above $60,000 \text{ K}$, but are also affected by $\log g$. Schönberner & Drilling also quote Bruhweiler et al. (1981) who showed that for the hot star HD 49798, lines of Fe V and to a lesser degree Fe IV, dominate the UV spectrum. For even hotter subdwarfs, such as BD+28°4211 ($T_{\text{eff}}=80,000 \text{ K}$) mainly lines of Fe VI dominate the UV, according to Dean and Bruhweiler (1985). Above $80,000 \text{ K}$ the Fe VII lines appear and above $100,000 \text{ K}$ Fe VI becomes less apparent. Thus, it is no surprise that Fe V lines were not detected in NGC 246. Only four definite, plus possibly two more, unblended Fe VI lines, in addition to five Fe VI lines that are blended with interstellar absorptions were detected. Moreover, the four Fe VII lines observable in the SWP range are also quite weak.

Some Fe VI absorptions are found in regions of strong, broad C IV and O VI absorptions, notably near the O VI $\lambda 1261$ trough that also contains interstellar S II $\lambda 1259$, Si II $\lambda 1260$, and a resonance mark. Three Fe VI lines, although strong by Fe VI standards (i.e., their intensities are given as 500–600 by Ekberg 1975b), contribute a negligible amount to the equivalent width of the broad O VI feature. A few Fe VI lines that are blended with interstellar or photospheric lines are also listed. Relative intensities for the Fe VI lines from Ekberg (1975b) are given in Column 8 of Table 1. We show the region near $\lambda 1261$ in Fig. 5 to illustrate that the deep absorption trough is mainly due to O VI. The isolated Fe VI line at $\lambda 1266.11$ has an EW of only 19 m\AA but is considered to be a strong line ($I=500$, Ekberg 1975b). Thus, the Fe VI lines of

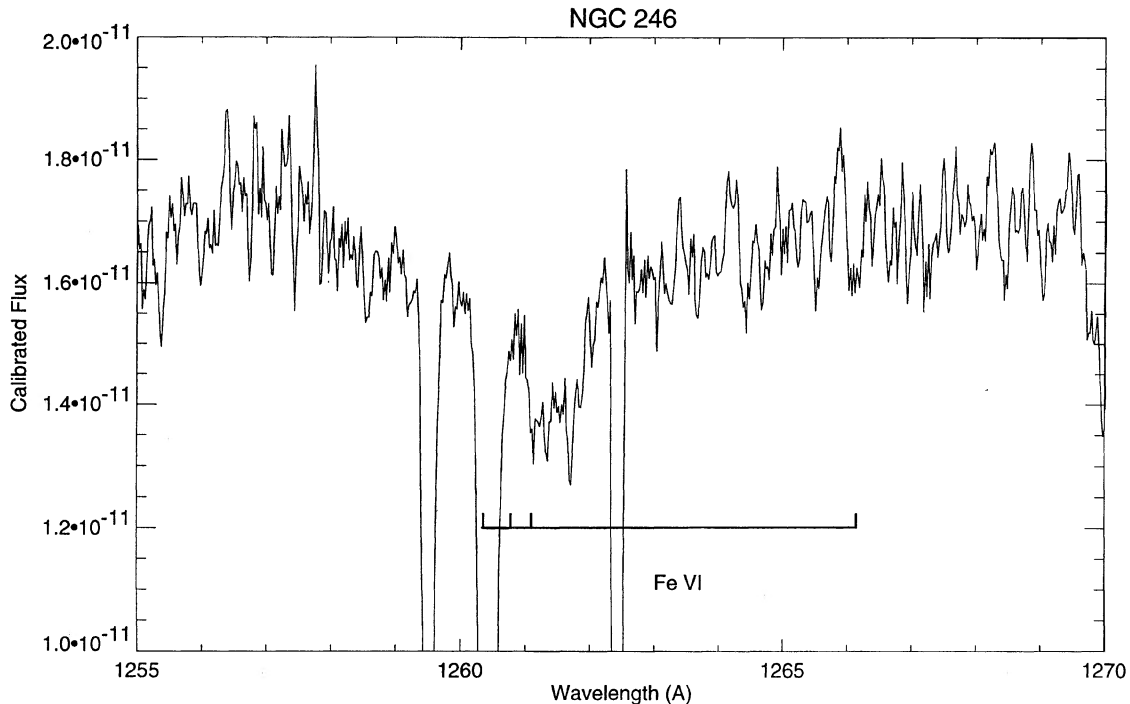


FIG. 5—Section of the spectrum of NGC 246 near the O VI $\lambda 1261$ absorption to show relative weakness of the "strong" Fe VI lines. The zero level has been depressed to show greater detail of the absorptions. The interstellar S II and Si II lines, as well as a resonance mark, are also present. Vertical tic marks show locations of four Fe VI rest wavelengths at $\lambda\lambda 1260.314, 1260.741, 1261.060,$ and 1266.103 , respectively.

comparable intensity at $\lambda\lambda 1260.314$, 1260.741 , and 1261.060 are overwhelmed by the strong O VI. Note that the zero level of Fig. 5 is depressed to show the comparative weakness of the Fe VI lines in more detail.

4.4 The Ne VII Absorption Lines

Werner and Rauch (1994) showed a plot of the UV Ne VII triplet from a single high-resolution *IUE* spectrum. Only a portion of the $\lambda 1992.1$ line was shown because of the 5 \AA interorder gap that was not treated by them. We show the region $\lambda 1980\text{--}\lambda 2000$ in Fig. 6 where the entire $\lambda 1992.1$ absorption is present, from the three best spectra, while the other lines are from nine coadded spectra. The measured equivalent widths of the Ne VII lines are in the ratio $\sim 3:3:2$, as compared to $6:3:1$ given in the laboratory work by Kelly (1987).

It is noteworthy to point out that the highly excited Ne VII lines show the greatest equivalent width for any unblended lines found in the SWP range.

4.5 The O V $\lambda 1371$ Line

The O V $\lambda 1371$ line is definitely present in the spectrum of NGC 246. A shortward shifted satellite line, pointed out by Sion et al. (1985) in the spectrum of PG 1034-001, appears to be present in NGC 246 as shown in Fig. 7 and is also seen in other very hot stars, such as Lo 5, RX J2117+3412, and PG 1159-035. For the latter, $T_{\text{eff}}=140,000 \text{ K}$ and $\log g=7$ was given by Werner et al. (1991).

4.6 The Interstellar Lines

Numerous interstellar lines (possibly with circumstellar contributions) are found in the SWP spectrum of NGC 246. They include strong lines of N I, S II, Si II, Si III, O I, C II, Fe II, Al II, and weak lines of C I and Al III. The Si III absorption at $\lambda 1206$ is resolved into three distinct components and the Si IV $\lambda 1393$ line has a secondary component, displaced by -9.1 km s^{-1} from the rest wavelength, similar to those seen for the C IV resonance doublet shown in Fig. 2.

4.7 The Radial Velocities

From the 11 strongest C IV absorptions we obtain a mean radial velocity of -23.6 km s^{-1} , in good agreement with a value of -24.8 km s^{-1} for the mean value of the four strongest O VI features. The image-numbers weighted (9:3:9) mean for the three Ne VII lines is -19.9 km s^{-1} and the single value for O V is -26.7 km s^{-1} . As mentioned in Sec. 4, the nominal error from a single spectrum is $\pm 3 \text{ km s}^{-1}$ so that one can expect a similar value for the coadded spectra.

The Fe VI lines are so weak that no exact value can be given for their radial velocity, except to state that for the few well-isolated (i.e., unblended, with $\text{EW} \approx > 7 \text{ m\AA}$) lines, the radial velocities are considerably less than for the strong species and average at about -3 km s^{-1} , about a factor of 8 less than the strong C IV and O VI lines. The Fe VII lines are even more questionable.

On the other hand, very good agreement is found for radial velocities of the strong resonance transitions: -66.5 and -63.3 km s^{-1} for N V, -67.7 and -70.4 km s^{-1} for Si IV, and -66.0 and -66.5 km s^{-1} for C IV.

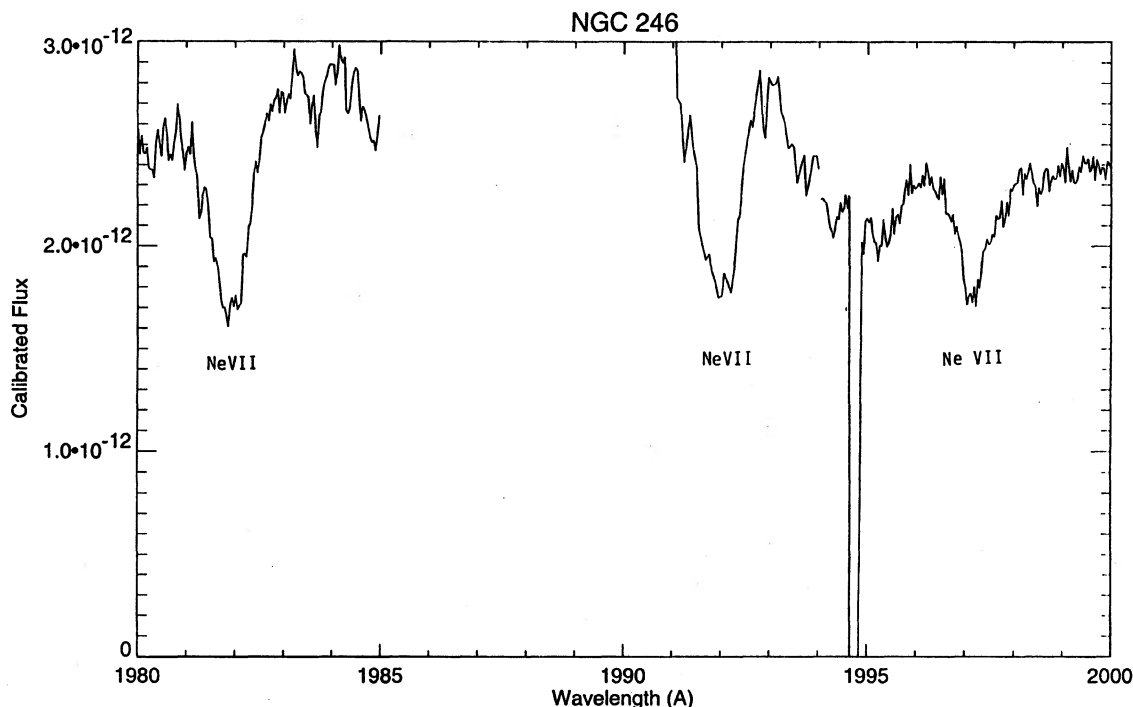


FIG. 6—Montage of the region $\lambda 1980\text{--}\lambda 2000$ for NGC 246, showing the strong Ne VII absorption lines. See Sec. 4.4 for more details.

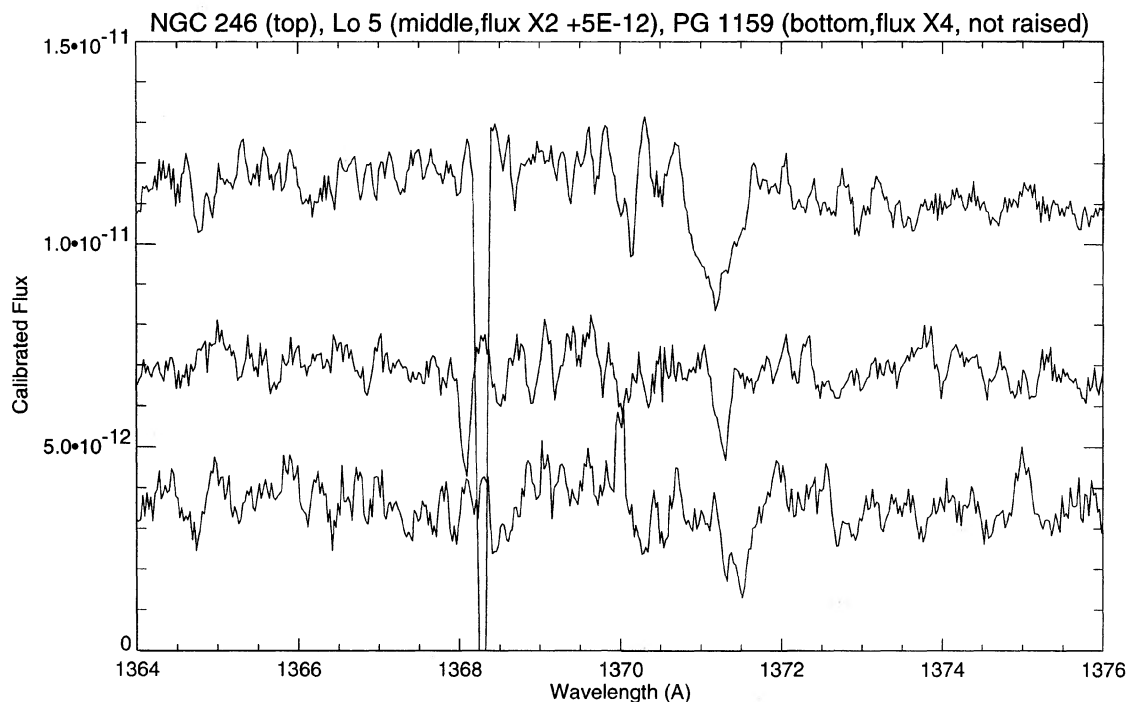


FIG. 7.—Multiplot of the O V absorption feature at $\lambda 1371$ seen in high-dispersion coadded spectra of NGC 246 (top, not raised). A shortward displaced satellite line appears to be present at $\lambda 1370.09$ with EW 35 Å. Middle tracing is for Lo 5 (flux multiplied by 2 and raised by $5E-12$), and bottom trace is for PG 1159–035 (flux X4, not raised). The plots are not adjusted for different radial velocities of the stars.

4.8 Some Unresolved Questions

A pair of fairly strong absorptions near $\lambda 1319$ remains unidentified. The sparsity of Fe VI and weakness of the Fe VII may be due to the extremely high T_{eff} of NGC 246 but it is also possible that this star does not possess a particularly high surface abundance of Fe. The peculiar shape of the C IV P Cyg profile is different from that normally seen in PNe. The nature of the companion line to O V $\lambda 1371$ needs clarification, if indeed it is O V, since Werner et al. (1991) have shown that O V is extremely sensitive to T_{eff} . A large number of absorption features with equivalent widths of less than 15 mÅ remain unidentified.

5. CONCLUSIONS

The major conclusions of this study are summarized as follows.

The *IUE* short wavelength (SWP) spectrum of the nucleus of NGC 246 is dominated by strong absorption lines of O V and C IV as is seen from the extensive line list. More than 75 transitions of C IV and O VI are identified, out of a total of about 140 absorption features that includes interstellar lines.

A higher S/N spectrum was obtained by coadding nine exposure-weighted high-resolution spectra. This number of spectra represents about the optimum for an improvement of \sqrt{n} ; for $n > 10$ information is lost.

The C IV resonance doublet is the only feature to exhibit a P Cygni profile from which a terminal wind velocity of $4120 \pm 200 \text{ km s}^{-1}$ was determined. The P Cyg profile is different from those normally found for PNe in that its deepest ab-

sorption is near v_{∞} . The narrow absorption features within the P Cyg profile each show a secondary component displaced by -10 km s^{-1} from the rest wavelengths while the main components are at -66 km s^{-1} .

For the strong C IV lines, a mean value of -23.6 km s^{-1} is obtained for their radial velocity, compared to a mean value of -24.8 km s^{-1} for the O VI lines.

The lines of the Ne VII triplet at $\lambda 1982.0$, 1992.1 , 1997.3 show the largest equivalent widths for any resolved lines in the UV spectrum of NGC 246, thus suggesting its neon-rich nature.

He II is not a major contributor to the blend of C IV and O VI lines near $\lambda 1640$.

No Fe V and few Fe VI lines were detected, and the four Fe VII lines are marginally observed.

An absorption feature near the $\lambda 1371$ O V line, thought to be an O V satellite line, needs further study since O V is extremely sensitive to T_{eff} .

Note added in Proof: O VI lines in NGC 246 were first reported by L. H. Allen in 1948 (ApJ, 108, 462).

I thank L. Taylor of the *IUE* Data Analysis Center (*IUEDAC*) for very helpful assistance and for generating the computer program to bridge the echelle interorder gap without which the spectra could not be coadded and the equivalent widths could not be determined in the $\lambda 1980$ – $\lambda 2000$ region, and F. Bruhweiler for making available the program TOTALPLOT to generate Fig. 1, as well as a careful reading of the manuscript and helpful discussions.

REFERENCES

- Acker, A., Ochsenbein, F., Stenholm, B., Tylenda, R., Marcout, R., and Schohn, C. 1992, *Strasbourg-ESO Catalogue of Galactic Planetary Nebulae* (Garching bei München, European Southern Observatory)
- Apparao, K. M. V., and Tarafdar, S. P. 1989, *ApJ*, 344, 826
- Bockasten, K., Hallin, R., and Hughes, T. P. 1963, *Proc. Phys. Soc.*, 81, 522
- Bruhweiler, F. C., Kondo, Y., and McCluskey, G. E. 1981, *ApJS*, 46, 255
- Dean, C. A., and Bruhweiler, F. C. 1985, *ApJS*, 57, 133
- Ekberg, O. 1975a, *Phys. Scripta*, 11, 23
- Ekberg, O. 1975b, *Phys. Scripta*, 12, 42
- Ekberg, O. 1981, *Phys. Scripta*, 23, 7
- Feibelman, W. A., and Johansson, S. 1995, *ApJS* (in press)
- Heap, S. R. 1982, in *Wolf-Rayet Stars: Observations, Physics, Evolution*, IAU Symp. 99, ed. C. W. H. de Loore and A. J. Willis, p. 423
- Husfeld, D. 1987, in *Second Conference on Faint Blue Stars*, IAU Colloq. 95, ed. A. G. D. Phillip, D. S. Hayes, and J. W. Liebert (Schenectady, NY, Davis)
- Kaler, J. B., Feibelman, W. A., and Henrichs, H. F. 1988, *ApJ*, 324, 528
- Kelly, R. L. 1987, *J. Phys. Chem. Ref. Data*, 16, Suppl.1, 155
- Morton, D. C. 1991, *ApJS*, 77, 119
- Schönberner, D., and Drilling, J. S. 1985, *ApJ*, 290, L49
- Sion, E. M., Liebert, J., and Wesemael, F. 1985, *ApJ*, 292, 477
- Smith, L. F., and Aller, L. H. 1969, *ApJ*, 157, 1245
- Werner, K., Heber, U., and Hunger, K. 1991, *A&A*, 244, 437
- Werner, K., and Rauch, T. 1994, *A&A*, 284, L5